# Uncertain Decision-Making Schemes for Knowledge-Based Anatomical Landmark Localization (K-BALL)*

M.-R. Siadat[a], H. Soltanian-Zadeh[a,b], and K. Elisevich[c]

[a]*Radiology Image Analysis Lab., Henry Ford Health System, Detroit, MI 48202, USA*
[b]*Department of Electrical and Computer Engineering, University of Tehran, Tehran 14395, Iran*
[c]*Department of Neurosurgery, Henry Ford Health System, Detroit, MI 48202, USA*

E-mails: siadat@rad.hfh.edu, hamids@rad.hfh.edu, nskoe@neuro.hfh.edu

***Abstract* – We have proposed a method for localization of anatomical landmarks comprised of two steps: 1) information extraction, and 2) information analysis. The focus of this paper is on the second step during which a set of points, found in the first step, is evaluated. This step utilizes a set of rules and eventually generates a confidence factor (*CNF*) for each set of points that indicates as to what degree they are good representatives of the "landmarks of interest." We also propose two alternative decision-making schemes: 1) Bayesian networks, and 2) possibilistic inference methods. The latter design is expected to outperform the other two as it utilizes both desired and undesired information. Our simulation study resulted in very similar performance for the rule-based and Bayesian schemes. The overall success rate (average of sensitivity and specificity) of the entire proposed method in localization of the hippocampus on MRI images was 83.3% with an accuracy of 99.2% (using rule-based decision-making scheme).**

## I. Introduction

Anatomical Landmark localization is important [1]-[2] as it provides: 1) initial information for registration, 2) navigation and retrieval guidance through the image data [3], 3) initial models for segmentation [4], and 4) valuable (though rough) information about the organs or structures of interest [3]. We have proposed a two-step knowledge-based method to localize lateral landmarks of the lateral ventricles, superior landmarks of the hippocampus, medial-inferior landmarks of the insular cortex [5]. This localization eventually provides a 3D deformable model with the initial model of the hippocampus. The steps involved in the proposed method are: 1) anatomical information extraction, and 2) information analysis. In this paper, we propose three frameworks for the second step: analysis of the spatial information extracted during the first step of the localization method. The proposed frameworks are based on: 1) rule-based systems, 2) Bayesian networks, and 3) possibilistic inference. We also propose a ground on which the proposed information analysis schemes can be evaluated in terms of their sensitivity, specificity, and overall success rate.

## II. Method

The localization method at the first step requires an expert to define a rough roadmap passing through a set of high-contrast landmarks (milestones), and eventually reaching at the structure of interest. The expert is asked to mark the milestones as desired points and a few points around them as undesired points. Then we estimate Gaussian models for the marked points and use them to determine the optimal search area for each desired landmark. The search areas estimated in this step are considered as segments of the statistical roadmap.

In the second step, we use the above statistical roadmap along with: 1) symmetry and 2) absolute statistical models to analyse the extracted anatomical information. The symmetry model indicates how symmetric the landmarks of interest extracted from the two hemispheres are relative to the interhemispheric plane. The absolute spatial model provides the distribution of landmarks of interest in a reference coordinates system (with roadmap starting point as its origin).

### *A. Information Extraction*

When localizing an anatomical structure, especially with low contrast and missing boundaries, the experts tend to look at the well-defined neighboring structures with high contrast to ensure that they have targeted the correct spot. This observation brings up the notion of making a roadmap to get to a desired anatomical landmark. A roadmap simply consists of a starting point and a few milestones with pre-specified segments taking us from one milestone to the next. Unlike the geographical maps, in an anatomical map the road from one landmark to the next one cannot be deterministically defined since it varies from subject to subject. So, we estimate a statistical map to optimize the sensitivity and specificity. There is an approximate geometrical position for each anatomical landmark, which can be looked for and found. An approximate relative spatial relationship does also exist among the anatomical structures. The above two postulations make it possible to build a statistical brain roadmap to localize the brain structures.

We use the expert-marked landmarks as the training set, (Fig. 1(a)) to estimate the statistical models of the desired and undesired landmarks (Fig. 1(c)). The undesired landmarks have similar features to those of the desired ones and are located in their close vicinities. Therefore, they can be deceitful and we should avoid them. Estimation of the optimal search areas and the search method (Fig. 1(b)) can be found in great details in our previous work [5].

*This work is partially supported by NIH Grant R01 EB002450.

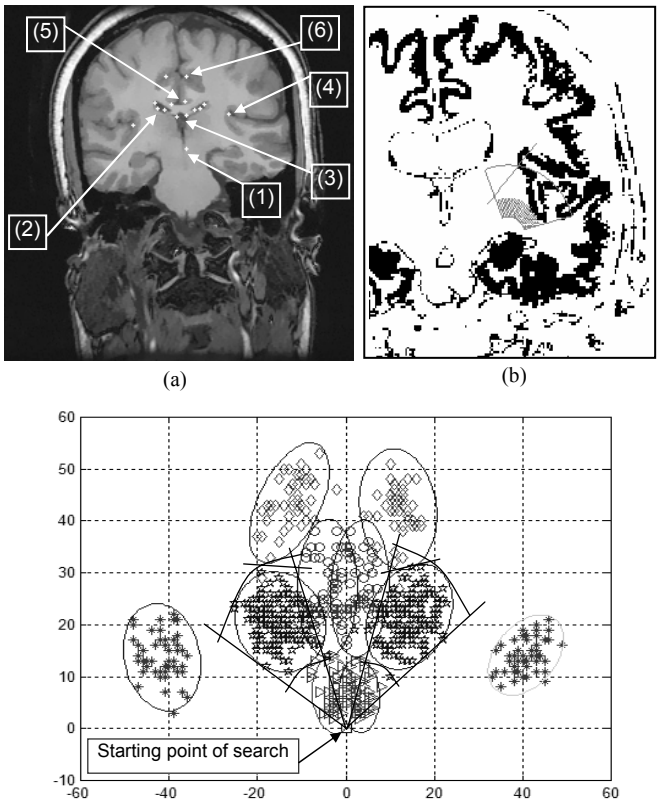


Fig. 1. a) Expert-marked landmarks for lateral ventricles when looking from starting point (point-1); lateral ventricles (point-2) as desired landmark, superior corners of third ventricle (point-3), medial points of Sylvian fissure (point-4), and lateral points of callosal sulcus (point-5) and eingulate sulcus (point-6) as undesired landmarks. b) Search performed on a GM map to find a point of insular cortex. c) Distribution of desired and undesired landmark points with isocontours drawn at 95% confidence level.

### *B. Information Analysis: Rule-Based System*

For this framework, we construct a set of fourteen rules using the estimated statistical models. We have defined three categories of rules based on: (*i*) absolute locations of the landmarks in a global reference coordinates system; (*ii*) relative locations of the landmarks; and (*iii*) general interhemispheric symmetry of the brain. The first category is based on our first postulation that the brain landmarks have absolute ballpark locations on the slices presenting the structure of interest. Furthermore, this ballpark location can be statistically modeled (in a global coordinates system built on the starting point of the search). So we estimate statistical models for absolute locations of the landmarks of interest using expert-marked landmarks very similar to the information extraction section. Fig. 2(a) depicts the points marked and the iso-contours of the models estimated in this regard. The iso-contours are determined at 95% confidence level that sets the probability of detection of the associated rules at 0.95. If a landmark is found in an unexpected region, i.e., outside of the iso-contour, the confidence of the system in correct identification of the landmark decreases.

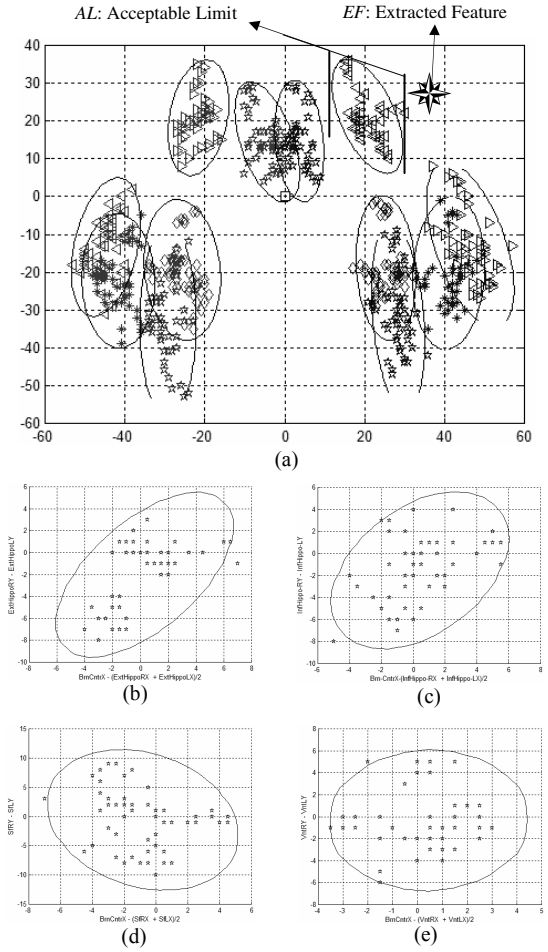


Fig. 2. a) Absolute coordinates of the lateral and medial points of the lateral ventricles (pentagrams and triangles, respectively), the superior, lateral, and inferior points of the hippocampus (diamonds, stars, and pentagrams, respectively), and the medial inferior points of the insular cortex (triangles). All the points are given in a reference coordinate system built on the roadmap's starting point as the origin. The iso-contours are drawn at 95% confidence level. (b)-(e) The deviations in vertical coordinate for each pair of a landmark at the left and right hemisphere vs. the deviation of the average of the corresponding horizontal coordinates from the interhemispheric plane, b) the lateral, c) the inferior landmarks of the hippocampus, d) the medial inferior points of the insular cortex, e) the lateral landmarks of the lateral ventricles.

For instance, a point found as the lateral landmark of the left lateral ventricle with a horizontal coordinate greater than 30 or less than 10 (called $EF_j$: *j*-th extracted features of the point) is not supported by the rule that corresponds to the absolute distribution of this landmark. This rule uses the above horizontal acceptable limits ($AL_{j,1}$ and $AL_{j,2}$) depicted in Fig. 2(a). These limits are violated by $EF_j$. In order to calculate the corresponding intermediate confidence factor ($ICNF_j$) we use the following formula:

$$ICNF_i = \begin{cases} 100 - \alpha_i & \alpha_i < 100 \\ 0 & \alpha_i > 100 \end{cases}$$

where $\alpha_i = \left( \sum_{\text{features of the } i-th \text{ rule}} (TP_{i,j} \times \min_k (EF_j - AL_{j,k}))^2 \right)^{0.5}$ and $TP_{i,j}$ is the softening parameter that governs a soft transition of the $i$-th rule based on an unacceptable mismatch in $j$-th $AL$ and $EF$. $TP$'s were mostly set to 10 in our work extending the transient strip to about 8 mm. A maximum $ICNF_i$ score of 100 strongly supports a found point and a minimum $ICNF_i$ score of zero strongly denies it to be what it is meant to be. A final confidence factor ($CNF$) is calculated as a sample mean of the $ICNF$'s. We consider the extracted landmarks reliable only when $CNF \geq 90$.

The second category considers the location of a brain structure relative to the other structures. In this case, a particular landmark is expected to be superior, inferior, medial, or lateral relative to another landmark. These qualitative expectations are converted to quantitative measures based on the statistical models (partly) shown in Fig. 2(a) as well as the ones derived in the information extraction section.

The third category is based on general symmetry of the brain. If MR images are acquired in coronal or axial directions, the symmetry feature will be observed relative to the interhemispheric plane. If there is a rotation toward the sagittal direction, this feature will not be valid any more. We materialize this relative symmetry concept in the proposed rules based on the statistical models derived here and partly shown in Fig. 2(b)-(e).

### C. *Information Analysis: Bayesian Network*

The proposed information analysis scheme, which can be considered as an extension of the conventional rule-based systems, performed well in our experiments with hippocampus initialization. However, it needs to calculate the acceptable limits and emphasizes the horizontal and vertical directions. Therefore, it is not the most efficient way of utilizing the statistical models. There are other information analysis methods (e.g., Bayesian networks and possibilistic inference). In the next two subsections, we briefly introduce the frameworks in which the information analysis phase can be extended starting with Bayesian networks and proceeding to possibilistic reasoning. Bayesian network is a natural extension of the scheme introduced in Subsection *B*. This comes from the fact that we can easily assign probability measures to each point found during the information extraction phase. As illustrated in Fig. 3, we may have a distribution model for the starting point of the roadmap in an anatomically defined coordinate system (e.g., anterior commissure-posterior commissure (AC-PC) segment). The Bayesian network then descends from its root node by calculating $P(St\_Pnt)$, the probability of correctly localizing the starting point of the roadmap. The next set of conditional probabilities, shown in Fig. 3, consists of evaluations of the extracted landmarks in their corresponding statistical models, i.e., $G_{d,i}(x,y)$ where $(x,y)$ is the coordinate of an extracted point and $G_{d,i}(x,y)$ is the Gaussian distribution of the $i$-th desired landmark. Note that $P(Ltr\_Vnt \mid St\_Pnt)$ is the probability of correctly localizing the lateral points of the lateral ventricles given the starting point of the roadmap is correctly localized. Similarly, $P(Sup\_Hippo \mid Ltr\_Vnt)$, $P(Inf\_Ins \mid Sup\_Hippo)$, $P(Inf\_Hippo \mid Sup\_Hippo)$, and $P(Ltr\_Hippo \mid Inf\_Ins)$ are the probabilities of correctly localizing the superior landmarks of the hippocampus, the inferior limit of the insular cortex, the inferior landmarks of the hippocampus, and lateral landmarks of the hippocampus given their conditions, respectively. These are all estimated in Subsection *A*. There are many branches in the network partially shown in Fig. 3. We are only interested in one path that results in the probabilities of localizing the desired landmarks correctly. These are shown in this figure by solid arrows. In particular, we are interested in two leaf nodes marked by rectangular boxes. Although $P(Sup\_Hippo \mid Ltr\_Vnt)$ is an important intermediate probability measure (marked with a rectangle), since it is a parent node and its value will eventually affect the child nodes (the probabilities are multiplied along each path of the tree), we do not need to directly consider it in the final CNF calculation. Using this scheme, we can substitute a major part of the relative rules with the proposed network. Therefore, in our final decision-making step ($CNF$ calculation) we combine these two leaf nodes as well as the $ICNF$ results produced by the remaining rules not covered by the proposed network.

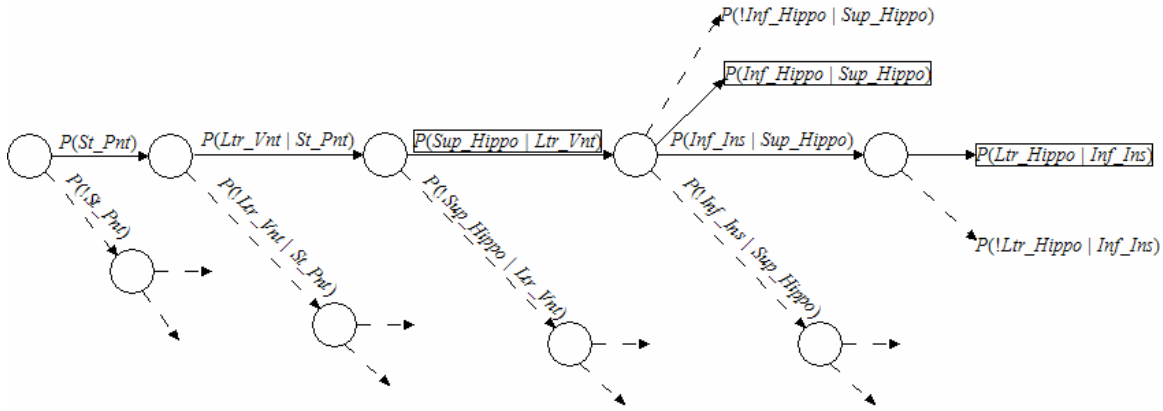


Fig. 3. Bayesian networks alternative for the information analysis phase that covers the category of relative rules.

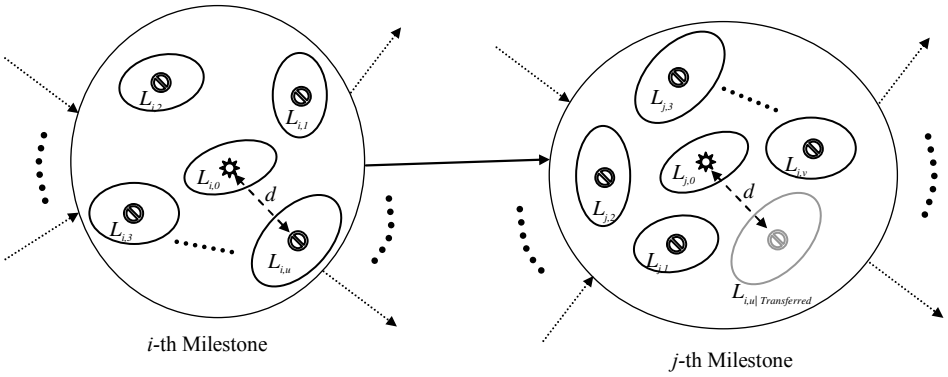


Fig. 4. Illustration of the notations and the way vagueness propagates through the roadmap segments, which is being modeled by the knowledge base. ✡ and ⊘ indicate the desired and undesired landmarks, respectively.

The other option would be to design similar networks for other categories of rules and investigate the way we could combine the results of each network or perhaps integrate different networks. It would be an interesting future work to implement and evaluate each of the above choices in a very well controlled simulation study.

*D. Information Analysis: Possibilistic Inference*

The previous extension of the proposed information analysis method, the Bayesian network, does not utilize the undesired models. Despite perfect tuning and efficient implementation, it is still not an optimal design, as it does not use all available information. The rationale for using the possibility measure is that in localizing natural (anatomical) landmarks, the landmarks of interest are not defined as a single point; rather, there is a range in which all points could be called a possible target point. For instance, there are several points any of which can be called a "superior landmark of hippocampus." Therefore, the possibility measures can model the situation more realistically. To build the possibility distributions ($\pi_i$'s), we can use the probabilistic models already estimated, truncate them at their 95% isocontours level and scale them so that value "one" would be assigned to every point inside an isocontour.

A universe $U = (\Omega^{(i)})_{i \in N_n}$ contains domains $\Omega^{(1)}, \ldots, \Omega^{(N_n)}$, belonging to each landmark of the roadmap with *n* landmarks. Each domain consists of the desired landmark and a set of undesired landmarks, i.e., $L_{i,h}$ corresponds to the possibility distribution of the *i*-th milestone of the roadmap where the desired and undesired landmarks correspond to $h = 0$ and $h \in \{1,\ldots,q\}$, respectively.

The knowledge base consists of a set of rules $R^{M_1}, \ldots, R^{M_m}$, corresponding to segments of the roadmap. If landmarks *i* and *j* are connected by a segment, an index set $M_k = \{i, j\} \in M$ will indicate this where *M* is defined as the set of all index sets and is called the modularization of $N_n$. We define $R^{M_k}$, the rule corresponding to $M_k$, as a matrix $R^{M_k} = [r_{u,v}]$, where,

$$r_{u,v} = \sup\{\inf(L_{i,u}|_{\bar{x}_{j,0}-\vec{d}}, L_{j,v})\}$$

The rationale behind this formulation is that as we deviate from the mean vector of the desired *i*-th landmark, the possibility of finding the next desired (i.e., *j*-th) landmark may change. The change has something to do with the distance, $\vec{d}$, by which we deviated from the *i*-th desired landmark. Fig. 4 illustrates how $q_i$ landmark of the *i*-th milestone is transferred into the *j*-th milestone coordinates and the way its possibility distribution interacts with the desired and undesired possibility distributions in these new coordinates. It is easy to see that when we are at the mean location of the *i*-th desired landmark, finding the *j*-th desired landmark is quite possible. This is a result of the proposed formula, i.e., $r_{0,0} = 1$.

$R(U,M) = \{R^{M_i} \mid M_i \in M\}$ is called a possibilistic rule base with regard to the universe, *U* and modularization, *M*. The following function:

$$\rho : \Omega \to [0,1],$$
$$\rho(\omega) = \min\left\{ext_{M_i}^{N_n}\left(R^{M_i}\right)(\omega) \mid M_i \in M\right\}$$

is called the possibilistic knowledge base induced by $R(U,M)$, which is considered non-contradictory if $\rho \in POSS(\Omega)$ holds.

The total evidence consists of evidences $E^{N_1}, \ldots, E^{N_n}$ corresponding to the milestones of the roadmap. The *i*-th piece of evidence, $E^{N_i} = \left(L_{i,0}(X_i), L_{i,1}(X_i), \ldots, L_{i,q_i}(X_i)\right)$, is produced by desired and undesired possibility distributions (models) of the *i*-th milestone using the *i*-th extracted landmark, $X_i$, as input to the possibilistic models, $L_{i,j}(.)$. $E(U,N) = \{E^{N_i} \mid N_i \in N,\ E^{N_i} \in POSS(\Omega^{N_i})\}$ is called a possibilistic evidence system with regard to universe, *U* and partition, *N*. Note that the partition determines the framework of our observations and, in our case, it is the set of all index sets of desired and undesired landmarks of each milestone. The following function:

$$\varepsilon : \Omega \to [0,1],$$
$$\varepsilon(\omega) = \min\left\{ext_{N_i}^{N_n}\left(E^{M_i}\right)(\omega) \mid N_i \in N\right\}$$

is called the total evidence induced by $E(U,M)$, which is considered non-contradictory if $\varepsilon \in POSS(\Omega)$ holds.

In classical applications of expert systems (e.g., [6]), the inference scheme is supposed to provide some information about the unobserved dimensions. It is unlikely that we will have observations (i.e., extracted points) at each and every dimension (milestone) of our universe. What we are interested in and planning to derive from the inference scheme is the propagation of uncertainty throughout the roadmap caused by intrinsically vague rules and imperfect information extractions. At this point, the state of the expert system, $\Phi$, is defined as:

$$\sigma(\Phi,\varepsilon(U,N)):\Omega\to[0,1],$$
$$\sigma(\Phi,\varepsilon(U,N))(\omega)=\min\{\rho(\omega),\varepsilon(\omega)\}$$

$\sigma$ is consistent if and only if it is a possibility distribution on $\Omega$. The possibility distribution $\kappa^{(i)}\in POSS(\Omega^{(i)})$ defined by $\kappa^{(i)}(\omega)=proj^{N_n}_{\{i\}}(\sigma(\Phi,\varepsilon(U,N)))(\omega)$ , $i=1,2,...,n,$ is called the *i*-th restriction of $\sigma(\Phi,\varepsilon(U,N))$ . It would be an interesting future work to see how the projections of the knowledge base on evidence indices, the raw evidences, and the restrictions, $\kappa^{(i)}$ , behave in a simulated environment where we have control on each part of the model. Having such a simulation, we could come up with a better idea whether we can solely depend on restrictions or we may combine them with raw evidences and the projections of the knowledge base on corresponding lower dimensions.

## III. Simulation and Experimental Results

We have simulated random vector $\boldsymbol{x}$, using white noise $\boldsymbol{w}$, as shown in block diagram of Fig. 5, by implementing $V\Lambda^{1/2}$ where V is the orthogonal matrix of eigenvectors of the covariance matrix of $\boldsymbol{x}$, $\Lambda$ is the diagonal matrix of corresponding eigenvalues, and $\boldsymbol{m_x}$ is the mean value of $\boldsymbol{x}$.

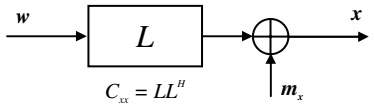


Fig. 5. Generating arbitrary random vector $\boldsymbol{x}$ from white noise $\boldsymbol{w}$.

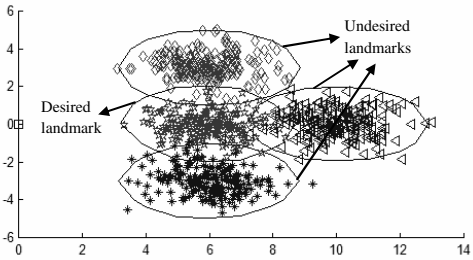


Fig. 6. One segment of the simulation with desired and undesired landmarks.

Fig. 6 Shows a simulated instance of a segment of the roadmap. Fig. 7 shows the false alarm rate as a function of two variables, *TP* and *CNF* threshold.

The rule-based and Bayesian method have performed similarly throughout our experiments with the simulation. However, we still need to further finetune our simulation and set up more distinct experiments to magnify the cons and pros of each method. We are planning to evaluate the proposed possibilistic inference, using this simulation.

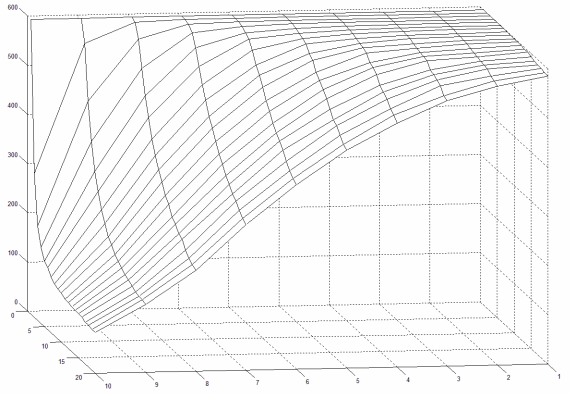

Fig. 7. False alarm rate vs. *TP* and *CNF* threshold.

We have applied the rule-based method on T1-weighted brain MRI of 10 epileptic patients to find the landmarks of the hippocampus. Two perpendicular views of the MRI data with the initial model overlaid on, are shown in Fig. 8. In our experiment, six patients formed the training set. The method made no false alarms. The overall success rate (average of sensitivity and specificity) of the algorithm was 83.3% with an accuracy of 99.2%.

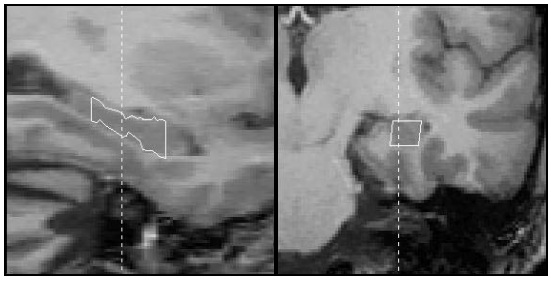

Fig. 8. Sagittal (left) and coronal (right) views of T1-weighted MRI with cross sections of initial models overlaid.

## References


[1] L. Verard, P. Allain, J.M. Travere, J. C. Baron, D. Bloyet, "Fully automatic identification of AC and PC landmarks on brain MRI using scene analysis," *IEEE Trans. on Medical Imaging*, vol. 16, no. 5, 1997.

[2] J. Cardillo, M.A. Sid-Ahmed, "An image processing system for locating craniofacial landmarks," *IEEE Trans. on Medical Imaging*, vol. 13, no. 2, 1994.

[3] M.-R. Siadat, H. Soltanian-Zadeh, F. Fotouhi, K. Elisevich, "Content-based image database system for epilepsy," *J. of Computer Methods and Programs in Biomedicine*, Elsevier Publisher, in press.

[4] A. Ghanei, H. Soltanian-Zadeh, "A discrete curvature-based deformable surface model with application to segmentation of volume images," *IEEE trans. on Information Technology in Biomedicine*, vol. 6, no. 4, 2002.

[5] M.-R. Siadat, H. Soltanian-Zadeh, F. Fotouhi, K. Elisevich, "Bayesian landmark identification in medical images," *SPIE*, vol. 5370, pp. 628-639, 2004.

[6] R. Kruse, J. Gebhardt, F. Klawonn, *Foundations of Fuzzy Systems*, John Willy & Sons, 1994.